Measurements of branching fractions and direct *CP* asymmetries for $B \to K\pi$, $B \to \pi\pi$ and $B \to KK$ decays

Y.-T. Duh,[30] T.-Y. Wu,[30] P. Chang,[30] G. B. Mohanty,[42] Y. Unno,[6] I. Adachi,[8] H. Aihara,[46] D. M. Asner,[35] V. Aulchenko,[1] T. Aushev,[13] T. Aziz,[42] A. M. Bakich,[41] B. Bhuyan,[9] M. Bischofberger,[27] A. Bondar,[1] G. Bonvicini,[51] A. Bozek,[31] M. Bračko,[23,14] T. E. Browder,[7] Y. Chao,[30] V. Chekelian,[53] A. Chen,[28] P. Chen,[30] B. G. Cheon,[6] R. Chistov,[13] I.-S. Cho,[52] K. Cho,[17] V. Chobanova,[53] Y. Choi,[40] Z. Doležal,[2] A. Drutskoy,[13] D. Dutta,[9] S. Eidelman,[1] H. Farhat,[51] J. E. Fast,[35] A. Frey,[5] V. Gaur,[42] R. Gillard,[51] Y. M. Goh,[6] B. Golob,[21,14] J. Haba,[8] K. Hayasaka,[26] H. Hayashii,[27] Y. Horii,[26] Y. Hoshi,[44] W.-S. Hou,[30] Y. B. Hsiung,[30] H. J. Hyun,[19] T. Iijima,[26,25] A. Ishikawa,[45] T. Julius,[24] J. H. Kang,[52] P. Kapusta,[31] T. Kawasaki,[33] H. J. Kim,[19] H. O. Kim,[19] J. H. Kim,[17] M. J. Kim,[19] Y. J. Kim,[17] K. Kinoshita,[3] B. R. Ko,[18] P. Kodyš,[2] S. Korpar,[23,14] P. Križan,[21,14] P. Krokovny,[1] T. Kuhr,[16] R. Kumar,[36] T. Kumita,[48] A. Kuzmin,[1] Y.-J. Kwon,[52] S.-H. Lee,[18] Y. Li,[50] J. Libby,[10] C. Liu,[38] Y. Liu,[3] K. Miyabayashi,[27] H. Miyata,[33] R. Mizuk,[13] T. Mori,[25] N. Muramatsu,[37] E. Nakano,[34] M. Nakao,[8] C. Ng,[46] S. Nishida,[8] K. Nishimura,[7] O. Nitoh,[49] S. Ogawa,[43] T. Ohshima,[25] S. Okuno,[15] S. L. Olsen,[39,7] G. Pakhlova,[13] H. Park,[19] H. K. Park,[19] T. K. Pedlar,[22] R. Pestotnik,[14] M. Petrič,[14] L. E. Piilonen,[50] M. Prim,[16] M. Ritter,[53] M. Röhrken,[16] S. Ryu,[39] H. Sahoo,[7] Y. Sakai,[8] S. Sandilya,[42] D. Santel,[3] Y. Sato,[45] O. Schneider,[20] C. Schwanda,[11] K. Senyo,[54] M. E. Sevior,[24] M. Shapkin,[12] V. Shebalin,[1] C. P. Shen,[25] T.-A. Shibata,[47] J.-G. Shiu,[30] B. Shwartz,[1] A. Sibidanov,[41] F. Simon,[53,55] P. Smerkol,[14] Y.-S. Sohn,[52] A. Sokolov,[12] E. Solovieva,[13] M. Starič,[14] M. Sumihama,[4] T. Sumiyoshi,[48] G. Tatishvili,[35] Y. Teramoto,[34] K. Trabelsi,[8] M. Uchida,[47] S. Uehara,[8] S. Uno,[8] P. Vanhoefer,[53] G. Varner,[7] A. Vinokurova,[1] C. H. Wang,[29] M.-Z. Wang,[30] M. Watanabe,[33] K. M. Williams,[50] E. Won,[18] B. D. Yabsley,[41] Y. Yamashita,[32] Z. P. Zhang,[38] V. Zhilich,[1] V. Zhulanov,[1] and A. Zupanc[16]

(The Belle Collaboration)

[1]*Budker Institute of Nuclear Physics SB RAS and Novosibirsk State University, Novosibirsk 630090*
[2]*Faculty of Mathematics and Physics, Charles University, Prague*
[3]*University of Cincinnati, Cincinnati, Ohio 45221*
[4]*Gifu University, Gifu*
[5]*II. Physikalisches Institut, Georg-August-Universität Göttingen, Göttingen*
[6]*Hanyang University, Seoul*
[7]*University of Hawaii, Honolulu 96822*
[8]*High Energy Accelerator Research Organization (KEK), Tsukuba*
[9]*Indian Institute of Technology Guwahati, Guwahati*
[10]*Indian Institute of Technology Madras, Madras*
[11]*Institute of High Energy Physics, Vienna*
[12]*Institute of High Energy Physics, Protvino*
[13]*Institute for Theoretical and Experimental Physics, Moscow*
[14]*J. Stefan Institute, Ljubljana*
[15]*Kanagawa University, Yokohama*
[16]*Institut für Experimentelle Kernphysik, Karlsruher Institut für Technologie, Karlsruhe*
[17]*Korea Institute of Science and Technology Information, Daejeon*
[18]*Korea University, Seoul*
[19]*Kyungpook National University, Taegu*
[20]*École Polytechnique Fédérale de Lausanne (EPFL), Lausanne*
[21]*Faculty of Mathematics and Physics, University of Ljubljana, Ljubljana*
[22]*Luther College, Decorah, Iowa 52101*
[23]*University of Maribor, Maribor*
[24]*School of Physics, University of Melbourne, Parkville, Victoria 3010*
[25]*Graduate School of Science, Nagoya University, Nagoya*
[26]*Kobayashi-Maskawa Institute, Nagoya University, Nagoya*
[27]*Nara Women's University, Nara*
[28]*National Central University, Chung-li*
[29]*National United University, Miao Li*
[30]*Department of Physics, National Taiwan University, Taipei*
[31]*H. Niewodniczanski Institute of Nuclear Physics, Krakow*
[32]*Nippon Dental University, Niigata*
[33]*Niigata University, Niigata*

^{34}*Osaka City University, Osaka*

^{35}*Pacific Northwest National Laboratory, Richland, Washington 99352*

^{36}*Panjab University, Chandigarh*

^{37}*Research Center for Electron Photon Science, Tohoku University, Sendai*

^{38}*University of Science and Technology of China, Hefei*

^{39}*Seoul National University, Seoul*

^{40}*Sungkyunkwan University, Suwon*

^{41}*School of Physics, University of Sydney, Sydney, New South Wales 2006*

^{42}*Tata Institute of Fundamental Research, Mumbai*

^{43}*Toho University, Funabashi*

^{44}*Tohoku Gakuin University, Tagajo*

^{45}*Tohoku University, Sendai*

^{46}*Department of Physics, University of Tokyo, Tokyo*

^{47}*Tokyo Institute of Technology, Tokyo*

^{48}*Tokyo Metropolitan University, Tokyo*

^{49}*Tokyo University of Agriculture and Technology, Tokyo*

^{50}*CNP, Virginia Polytechnic Institute and State University, Blacksburg, Virginia 24061*

^{51}*Wayne State University, Detroit, Michigan 48202*

^{52}*Yonsei University, Seoul*

^{53}*Max-Planck-Institut für Physik, München*

^{54}*Yamagata University, Yamagata*

^{55}*Excellence Cluster Universe, Technische Universität München, Garching*

We report measurements of the branching fractions and direct CP asymmetries ($\mathcal{A}_{CP}$) for $B \to K\pi$, $\pi\pi$ and KK decays (but not $\pi^0\pi^0$) based on the final data sample of 772×10^6 $B\bar{B}$ pairs collected at the $\Upsilon(4S)$ resonance with the Belle detector at the KEKB asymmetric-energy e^+e^- collider. We set a 90% confidence-level upper limit for K^+K^- at 2.0×10^{-7}; all other decays are observed with branching fractions ranging from 10^{-6} to 10^{-5}. In the $B^0/\bar{B}^0 \to K^\pm\pi^\mp$ mode, we confirm Belle's previously reported large $\mathcal{A}_{CP}$ with a value of $-0.069 \pm 0.014 \pm 0.007$ and a significance of 4.4σ. For all other flavor-specific modes, we find $\mathcal{A}_{CP}$ values consistent with zero, including $\mathcal{A}_{CP}(K^+\pi^0) = +0.043 \pm 0.024 \pm 0.007$ with 1.8σ significance. The difference of CP asymmetry between $B^\pm \to K^\pm\pi^0$ and $B^0/\bar{B}^0 \to K^\pm\pi^\mp$ is found to be $\Delta\mathcal{A}_{K\pi} \equiv \mathcal{A}_{CP}(K^+\pi^0) - \mathcal{A}_{CP}(K^+\pi^-) = +0.112 \pm 0.027 \pm 0.007$ with 4.0σ significance. We also calculate the ratios of partial widths for the $B \to K\pi$ decays. Using our results, we test the validity of the sum rule $\mathcal{A}_{CP}(K^+\pi^-) + \mathcal{A}_{CP}(K^0\pi^+)\frac{\Gamma(K^0\pi^+)}{\Gamma(K^+\pi^-)} - \mathcal{A}_{CP}(K^+\pi^0)\frac{2\Gamma(K^+\pi^0)}{\Gamma(K^+\pi^-)} - \mathcal{A}_{CP}(K^0\pi^0)\frac{2\Gamma(K^0\pi^0)}{\Gamma(K^+\pi^-)} = 0$ and obtain a sum of $-0.270 \pm 0.132 \pm 0.060$ with 1.9σ significance.

Charmless B meson decays to $K\pi$, $\pi\pi$ and KK final states provide a good test bed to understand B decay mechanisms and to search for physics beyond the Standard Model (SM). Although predictions for the branching fractions under various theoretical approaches suffer from large hadronic uncertainties, direct CP asymmetries and ratios of branching fractions can still provide excellent sensitivity to new physics (NP), since many theoretical and experimental uncertainties cancel out in these quantities. The direct CP asymmetry is defined as

$$\mathcal{A}_{CP} \equiv \frac{N(\bar{B} \to \bar{f}) - N(B \to f)}{N(\bar{B} \to \bar{f}) + N(B \to f)}, \quad (1)$$

where $f/\bar{f}$ denotes a specific final state from a B^+/B^- or $B^0/\bar{B}^0$ decay. For instance, the observed $\mathcal{A}_{CP}$ difference between $B^\pm \to K^\pm\pi^0$ and $B^0/\bar{B}^0 \to K^\pm\pi^\mp$ [1–3], also known as the $\Delta\mathcal{A}_{K\pi}$ puzzle, can be explained by an enhanced color-suppressed tree contribution [4] or NP in the electroweak penguin loop [5]. Other variables sensitive

to electroweak penguin contributions are the ratios of partial widths, e.g., $R_c \equiv 2\Gamma(B^+ \to K^+\pi^0)/\Gamma(B^+ \to K^0\pi^+)$ and $R_n \equiv \Gamma(B^0 \to K^+\pi^-)/2\Gamma(B^0 \to K^0\pi^0)$. Prior measurements [3,6–8] of these ratios are consistent with theory expectations [9–12], albeit with large errors. The experimental uncertainties, therefore, need to be improved to adequately compare data and SM predictions.

In this paper, we report measurements of the branching fractions for $B \to K\pi$, $\pi\pi$, and KK decays, other than $B^0 \to \pi^0\pi^0$, and of the direct CP asymmetries for the modes with flavor-specific final states [13]. The measurements are based on 772×10^6 $B\bar{B}$ pairs, corresponding to the final $\Upsilon(4S)$ data set collected with the Belle detector [14] at the KEKB e^+e^- asymmetric-energy collider [15]. Compared to our previous publications [1,6,16], we have increased the KK, $K^0\pi^+$ and $\pi^+\pi^-$ data samples by about 72%, the $K^+\pi^-$, $K^+\pi^0$ and $\pi^+\pi^0$ samples by about 44%, and the $K^0\pi^0$ sample by about 18%, have included several improvements in reconstruction algorithms that enhance

the reconstruction efficiency for the charged tracks, and have made numerous modifications to the analysis to improve the measurement sensitivity [e.g., by including an extra discriminating variable in the likelihood fit; see Eq. (2)].

We define our event selection criteria for these measurements as follows. Charged tracks originating from a B decay are required to have a distance of closest approach with respect to the interaction point less than 4.0 cm along the beam direction (z-axis) and less than 0.3 cm in the transverse plane. Charged kaons and pions are identified with information from particle identification detectors, which are combined to form a K-π likelihood ratio $\mathcal{R}_{K/\pi} = \mathcal{L}_K/(\mathcal{L}_K + \mathcal{L}_\pi)$, where $\mathcal{L}_K$ ($\mathcal{L}_\pi$) is the likelihood of the track being a kaon (pion). Track candidates with $\mathcal{R}_{K/\pi} > 0.6$ (<0.4) are classified as kaons (pions). The typical kaon (pion) identification efficiency is 83% (88%) with a pion (kaon) misidentification probability of 7% (11%). A tighter $\mathcal{R}_{K/\pi}$ requirement (> 0.7) is applied for the $\bar{K}^0 K^+$ channel to reduce the $B^+ \rightarrow K^0 \pi^+$ feed-across since the $\bar{K}^0 K^+$ branching fraction is an order of magnitude smaller than that of $K^0 \pi^+$. Charged tracks found to be consistent with an electron or a muon are rejected. Candidate K^0 mesons are reconstructed via $K_S^0 \rightarrow \pi^+ \pi^-$ [17] by requiring the invariant mass of the pion pair to be 480 MeV/c^2 < $M_{\pi\pi}$ < 516 MeV/c^2 (corresponding to 5.2σ around the mean value). Pairs of photons with invariant masses lying in the range of 115 MeV/c^2 < $M_{\gamma\gamma}$ < 152 MeV/c^2 (corresponding to 2.5σ around the mean value) are classified as π^0 candidates. The photon energy is required to be greater than 50 (100) MeV in the barrel (endcap) calorimeter.

Candidate B mesons are identified using the beam-energy-constrained mass, $M_{\rm bc} \equiv \sqrt{E_{\rm beam}^{*2}/c^4 - |\vec{p}_B^{\,*}/c|^2}$, and the energy difference, $\Delta E \equiv E_B^* - E_{\rm beam}^*$, where $E_{\rm beam}^*$ is the run-dependent beam energy, and E_B^* and p_B^* are the reconstructed energy and momentum of B candidates in the center-of-mass (CM) frame, respectively. Events with $M_{\rm bc} > 5.2$ GeV/c^2 and $|\Delta E| < 0.3$ GeV are retained for further analysis. For decays having a π^0 in the final state, the correlation between $M_{\rm bc}$ and ΔE is relatively large due to photon shower leakage in the calorimeter. To reduce this correlation, $M_{\rm bc}$ is calculated by scaling the measured π^0 momentum to the value expected for signal, given by $\vec{p}_{\pi^0}^{\,*} = \frac{\vec{p}_{\pi^0}^{\,*}}{|\vec{p}_{\pi^0}^{\,*}|}\sqrt{(E_{\rm beam}^* - E_{h^\pm}^*)^2/c^2 - m_{\pi^0}^{*2}c^2}$, where $h^\pm$ represents the charged kaon or pion. Consequently, the correlation coefficient falls from +18% to −4%, as shown by a Monte Carlo (MC) study.

The dominant background arises from $e^+ e^- \rightarrow q\bar{q}$ ($q = u, d, s, c$) continuum events. We use event topology to distinguish spherical $B\bar{B}$ events from the jet-like continuum background. A set of modified Fox-Wolfram moments [18] is combined into a Fisher discriminant. Signal and background likelihoods are formed based on

MC events. The likelihood, $\mathcal{L}$, is the product of the probability density functions (PDFs) for the Fisher discriminant, the cosine of the polar angle of the B-meson flight direction in the CM frame, and the flight-length difference (Δz) along the z-axis between the decay vertex of the signal B and the vertex formed from the tracks not associated with the signal B. The decay vertices for $B^+ \rightarrow h^+ h^0$ (where h^0 represents π^0 or K^0) candidates are estimated by the point of closest approach of the h^+ trajectory to the z-axis. Since the $K^0 \pi^0$ mode has no primary charged track, the Δz variable is not used. A loose continuum suppression requirement of $\mathcal{R} > 0.2$ rejects more than 70% of the background, where $\mathcal{R} = \mathcal{L}_{\rm sig}/(\mathcal{L}_{\rm sig} + \mathcal{L}_{q\bar{q}})$ and $\mathcal{L}_{\rm sig}$ ($\mathcal{L}_{q\bar{q}}$) is the signal (continuum) likelihood. The variable $\mathcal{R}$ is then transformed to $\mathcal{R}' \equiv \ln(\frac{\mathcal{R}-0.2}{1.0-\mathcal{R}})$, whose distribution for signal or backgrounds is easily modeled by analytical functions.

Background contributions from $\Upsilon(4S) \rightarrow B\bar{B}$ events are investigated with large MC samples that include B decays to final states with and without charm mesons. After all selection requirements are imposed, backgrounds with charm mesons are found to be negligible; charmless backgrounds from multibody B decays are present at negative ΔE values. We also identify feed-across backgrounds from other $B \rightarrow hh$ channels, which are typically shifted by 45 MeV in ΔE due to K-π misidentification.

Signal yields are extracted by performing unbinned extended maximum likelihood fits to the ($M_{\rm bc}$, ΔE, $\mathcal{R}'$) distributions of the candidates. The likelihood function for each mode is

$$\mathcal{L} = e^{-\sum_j N_j} \times \prod_i \left(\sum_j N_j \mathcal{P}_j^i\right), \quad \text{where}$$

$$\mathcal{P}_j^i = \frac{1}{2}[1 - q^i \cdot \mathcal{A}_{CP,j}]\mathcal{P}_j(M_{\rm bc}^i, \Delta E^i, \mathcal{R}'^i).$$

(2)

Here, i is the event index and N_j is the yield of events for the category j, which indexes signal, continuum, feed-across, and other charmless B decays. $\mathcal{P}_j(M_{\rm bc}^i, \Delta E^i, \mathcal{R}'^i)$ is the PDF in $M_{\rm bc}$, ΔE, and $\mathcal{R}'$ for the ith event. The flavor q of the B-meson candidate is +1 (−1) for B^+ and B^0 (B^- and $\bar{B}^0$); $\mathcal{A}_{CP,j}$ is the direct CP asymmetry for category j. For CP specific modes, $\mathcal{P}_j^i$ in Eq. (1) is simply $\mathcal{P}_j(M_{\rm bc}^i, \Delta E^i, \mathcal{R}'^i)$. The validity of the three-dimensional fit is checked by large ensemble tests using MC events and studies of data in high statistics control samples of $B^+ \rightarrow \bar{D}^0(K^+\pi^-)\pi^+$ and $B^+ \rightarrow \bar{D}^0(K^+\pi^-\pi^0)\pi^+$ decays. The measured branching fractions for the control samples are consistent with the corresponding world-average values [19]. Our transition to a three-dimensional fit, compared to the two-dimensional fit of previous publications [1,6], results in an effective gain in luminosity of 32%, 33% and 466% [20] for $B \rightarrow K^+\pi^-$, $K^+\pi^0$ and K^+K^- decays, respectively, as evaluated by ensemble tests.

We perform three separate simultaneous fits for pairs of modes that feed across into each other: (a) $B^0 \to K^+\pi^-$ and $B^0 \to \pi^+\pi^-$, (b) $B^+ \to K^+\pi^0$ and $B^+ \to \pi^+\pi^0$, and (c) $B^+ \to K^0\pi^+$ and $B^+ \to \bar{K}^0K^+$. For these fits, feed-across fractions are constrained according to the identification efficiencies and misidentification probabilities of charged kaons and pions. The $B^0 \to K^+K^-$ channel is fitted alone, with the $B^0 \to K^+\pi^-$ branching fraction fixed to the value obtained from fit (a). The $K^0\pi^0$ and $K^0\bar{K}^0$ channels are fitted independently, as they have no feed-across contribution from other modes.

The PDFs for signal and feed-across are modeled in $M_{\rm bc}$ with a single Gaussian function, in ΔE with a Crystal Ball function [21] (a double Gaussian function) for the modes with (without) a π^0, and in $\mathcal{R}'$ with a double or triple Gaussian function. Since large signals are expected for $B^0 \to K^+\pi^-$, $\pi^+\pi^-$, and $K^0\pi^+$ decays, both the means and widths for $M_{\rm bc}$, ΔE and $\mathcal{R}'$ are floated in the fit. For the three $h\pi^0$ modes, the $M_{\rm bc}$ means and widths are allowed to vary; the ΔE means are also floated while assuming the same shift relative to MC values; the $\mathcal{R}'$ means and widths as well as the ΔE widths are fixed to MC values after calibrating for the data-MC differences as evaluated with control samples [22,23]. For the low-statistics $B^+ \to \bar{K}^0K^+$ decay, the means and widths for $M_{\rm bc}$, ΔE and $\mathcal{R}'$ are scaled by the relative positions and constant factors with respect to the parameters of $B^+ \to K^0\pi^+$. For the $K^0\bar{K}^0$ mode, all parameters of signal PDFs are first fixed to MC values and then adjusted according to calibration factors obtained with the control sample [23]. In the $B^0 \to K^+K^-$ fit, a triple Gaussian function is used to model the large amount of feed-across from $B^0 \to K^+\pi^-$, which includes a ΔE tail. The means and widths for K^+K^- PDFs are scaled by the relative values with respect to floating $K^+\pi^-$ parameters.

The continuum background PDF is described by the product of a first- or a second-order Chebyshev polynomial for ΔE, an ARGUS function [24] for $M_{\rm bc}$, and a double Gaussian function for $\mathcal{R}'$, modeled using off-resonance data. The ΔE shape coefficients, the ARGUS slope parameter, and the $\mathcal{R}'$ mean and width are free parameters in the fit. A slight correlation ($|r_{ij}| < 3\%$) between the ΔE shape coefficients and $\mathcal{R}'$ is found in continuum events. Therefore, the continuum ΔE shape coefficients are allowed to vary in four different $\mathcal{R}'$ regions. For charmless B backgrounds, a two-dimensional histogram is used for $(M_{\rm bc}, \Delta E)$ to account for the correlation between these variables, while a double Gaussian function is employed for $\mathcal{R}'$.

Projections of the fit in $M_{\rm bc}$ and ΔE are shown in Figs. 1 and 2, while projections in $\mathcal{R}'$ can be found in Ref. [25]. Table I summarizes the fit results for all modes. Assuming the production rates of B^+B^- and $B^0\bar{B}^0$ pairs to be equal at the $\Upsilon(4S)$ resonance, the branching fraction for each mode is calculated by dividing the fitted signal yield by the number of $B\bar{B}$ pairs and the reconstruction efficiency.
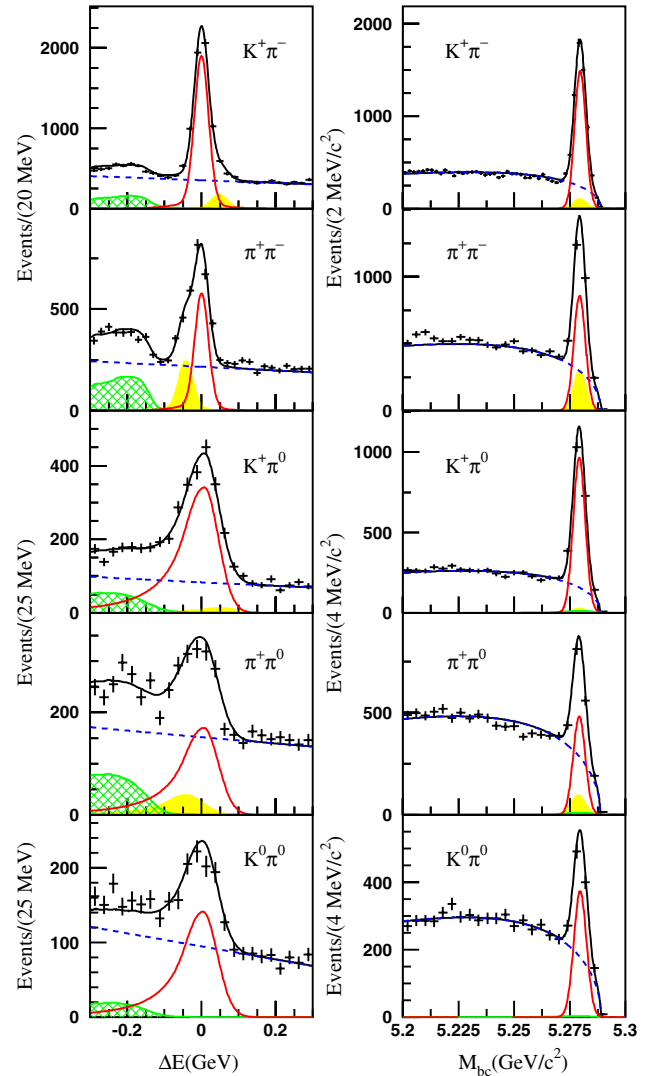

FIG. 1 (color online). ΔE (left) and $M_{\rm bc}$ (right) distributions for $B^0 \to K^+\pi^-$, $B^0 \to \pi^+\pi^-$, $B^+ \to K^+\pi^0$, $B^+ \to \pi^+\pi^0$ and $B^0 \to K^0\pi^0$ candidates. Points with error bars represent the data, while the curves denote various components of the fit: signal (solid red), continuum (dashed blue), charmless B background (hatched green), background from misidentification (filled yellow), and sum of all components (solid black). The ΔE and $M_{\rm bc}$ projections of the fits are for events in the $\mathcal{R}'$ signal enhanced region ($\mathcal{R}' > 1.47$ for $K^+\pi^-$, $\pi^+\pi^-$, and $K^0\pi^0$; $\mathcal{R}' > 2.71$ for others) and $M_{\rm bc} > 5.27$ GeV/c^2 or $-0.14(-0.06)$ GeV $< \Delta E < 0.06$ GeV with (without) a π^0 in the final state.

Significant signals are observed in all channels except $B^0 \to K^+K^-$ (which has 1.2σ significance). An upper limit at 90% confidence level on the branching fraction for this mode is obtained by integrating the likelihood distribution, which is convolved with a Gaussian function whose width equals the systematic uncertainty.

The fitting systematic uncertainties are due to signal PDF modeling, feed-across constraints and charmless B background modeling. The PDF modeling uncertainties are estimated from the differences in signal yields while
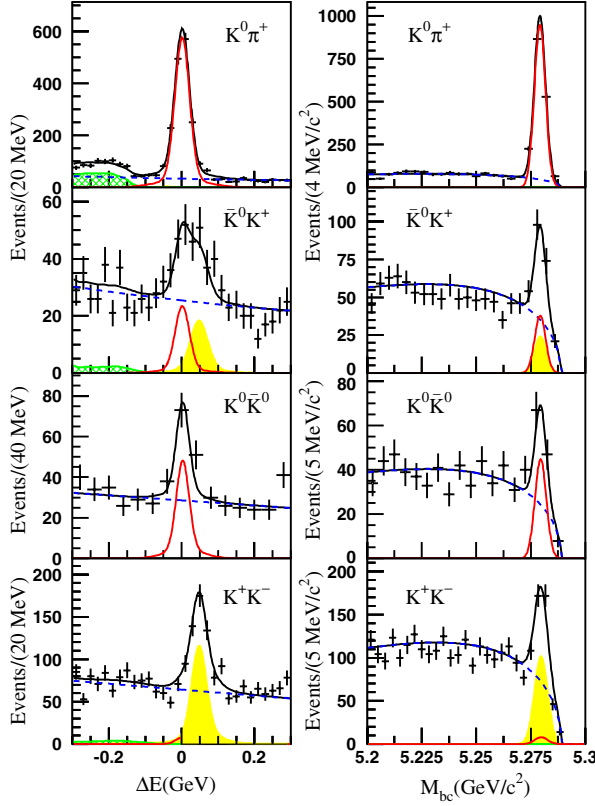
FIG. 2 (color online). ΔE (left) and M_{bc} (right) distributions for $B^+ \to K^0\pi^+$, $B^+ \to \bar{K}^0 K^+$, $B^0 \to K^0\bar{K}^0$ and $B^0 \to K^+K^-$ candidates. The selections for fit projections and PDF component descriptions are identical to those in Fig. 1 ($\mathcal{R}' > 1.47$ for $K^0\bar{K}^0$; $\mathcal{R}' > 2.71$ for others).

varying the calibration factors of signal PDFs by one standard deviation. The uncertainty that arises from the modeling of final state radiation (FSR) is determined by lowering the photon energy threshold in PHOTOS [27] from 26 MeV (default) to 2.6 MeV to derive a new set of signal PDFs, and subsequently a new fitted yield. For $h^+\pi^0$ modes, the latter uncertainties are negligible since photon

shower leakage in the calorimeter causes a much larger ΔE tail than FSR. Uncertainties in K-π misidentification probabilities and fractions of feed-across events account for the dominant systematic uncertainty of 42.17% in the $B^0 \to K^+K^-$ channel, and 0.18% to 2.28% for the other modes. Also a 0.45% fitting bias for $B^0 \to K^+\pi^-$ is incorporated by taking half of the yield deviation ratio in ensemble tests with the simultaneous fit. The systematic uncertainties due to charmless B backgrounds are evaluated by measuring the difference in the fitted yield after changing the fitting region to $\Delta E > -0.12$ GeV. The above deviations in the signal yield are added in quadrature to obtain the overall systematic error due to fitting.

The systematic error in efficiency caused by the likelihood ratio cut, $\mathcal{R} > 0.2$, is investigated using control samples [23]. The systematic uncertainty due to charged-track reconstruction efficiency is estimated to be 0.35% per track using partially reconstructed $D^{*+} \to D^0(\pi^+\pi^-\pi^0)\pi^+$ events. The systematic uncertainty due to the $\mathcal{R}_{K/\pi}$ selection, which is around 0.8% for kaons and 0.9% for pions, is determined from a study of the $D^{*+} \to D^0(K^-\pi^+)\pi^+$ sample; the systematic uncertainties on K_S^0 and π^0 reconstruction are studied using the $D^* \to D^0(K_S^0\pi^+\pi^-)\pi$ sample and the yield ratio between $\eta \to \pi^0\pi^0\pi^0$ and $\eta \to \pi^+\pi^-\pi^0$, respectively. The systematic uncertainty due to the error on the total number of $B\bar{B}$ pairs is 1.37% [28]. The uncertainty due to signal MC statistics is 0.2%. The final systematic uncertainty is obtained by summing all these contributions in quadrature and Table II summarizes all the systematic uncertainties.

Out of the five flavor-specific decay modes presented in Table I, clear evidence for direct CP asymmetry is found only in the $B^0 \to K^+\pi^-$ channel. The $\mathcal{A}_{CP}$ systematic errors due to fitting are estimated with the same procedure as applied for the branching fractions. Possible detector bias due to tracking acceptance and $\mathcal{R}_{K/\pi}$ selection for $h^0\pi^+$ modes are evaluated using the measured $\mathcal{A}_{CP}$ values from the continuum. Since there is a negligible proton contamination arising from p-π misidentification in the

TABLE I. Signal yields, product of efficiencies (ε) and sub-decay branching fractions ($\mathcal{B}_s$) [26], measured branching fractions ($\mathcal{B}$), direct CP asymmetries ($\mathcal{A}_{CP}$) after the correction, and significance of CP asymmetries ($\mathcal{S}$) for individual modes. The first and second quoted errors are statistical and systematic, respectively. Upper limit is given at the 90% confidence level.

Mode	Yield	$\varepsilon \times \mathcal{B}_s$(%)	$\mathcal{B}(10^{-6})$	$\mathcal{A}_{CP}$	$\mathcal{S}(\sigma)$
$K^+\pi^-$	7525 ± 127	48.82	$20.00 \pm 0.34 \pm 0.60$	$-0.069 \pm 0.014 \pm 0.007$	4.4
$\pi^+\pi^-$	2111 ± 89	54.79	$5.04 \pm 0.21 \pm 0.18$	$\cdots$	$\cdots$
$K^+\pi^0$	3731 ± 92	38.30	$12.62 \pm 0.31 \pm 0.56$	$+0.043 \pm 0.024 \pm 0.002$	1.8
$\pi^+\pi^0$	1846 ± 82	40.80	$5.86 \pm 0.26 \pm 0.38$	$+0.025 \pm 0.043 \pm 0.007$	0.6
$\bar{K}^0 K^+$	134 ± 23	15.64	$1.11 \pm 0.19 \pm 0.05$	$+0.014 \pm 0.168 \pm 0.002$	0.1
$K^0\pi^+$	3229 ± 71	17.46	$23.97 \pm 0.53 \pm 0.71$	$-0.011 \pm 0.021 \pm 0.006$	0.5
$K^0\bar{K}^0$	103 ± 15	10.61	$1.26 \pm 0.19 \pm 0.05$	$\cdots$	$\cdots$
$K^0\pi^0$	961 ± 45	12.86	$9.68 \pm 0.46 \pm 0.50$	$\cdots$	$\cdots$
K^+K^-	35 ± 29	47.72	$0.10 \pm 0.08 \pm 0.04(<0.20)$	$\cdots$	$\cdots$

TABLE II.   Systematic uncertainties (%) on the measured branching fractions of $B \to hh$.

Source	$K^+\pi^-$	$\pi^+\pi^-$	$K^+\pi^0$	$\pi^+\pi^0$	$\bar{K}^0K^+$	$K^0\pi^+$	$K^0\bar{K}^0$	$K^0\pi^0$	K^+K^-
Tracking	0.70	0.70	0.35	0.35	0.35	0.35	$\cdots$	$\cdots$	0.70
$\mathcal{R}_{K/\pi}$	1.65	1.72	0.78	0.86	0.80	0.86	$\cdots$	$\cdots$	1.58
$\mathcal{R} > 0.2$	0.55	0.24	0.59	0.92	0.91	0.80	0.84	1.04	0.28
MC statistics	0.16	0.15	0.18	0.17	0.20	0.19	0.24	0.23	0.16
$N_{B\bar{B}}$	1.37	1.37	1.37	1.37	1.37	1.37	1.37	1.37	1.37
π^0	$\cdots$	$\cdots$	4.0	4.0	$\cdots$	$\cdots$	$\cdots$	4.0	$\cdots$
K_S^0	$\cdots$	$\cdots$	$\cdots$	$\cdots$	1.68	1.68	3.36	1.68	$\cdots$
Signal PDF	0.28	$+0.49$ -0.51	0.43	$+0.89$ -0.66	$+0.64$ -0.63	0.18	$+1.02$ -1.00	1.80	$+6.76$ -5.16
Feed-across	0.49	$+1.30$ -1.80	0.42	1.19	$+2.28$ -2.25	0.18	$\cdots$	$\cdots$	42.17
Fitting bias	0.45	$\cdots$	$\cdots$	$\cdots$	$\cdots$	$\cdots$	$\cdots$	$\cdots$	$\cdots$
PHOTOS	1.2	0.8	$\cdots$	$\cdots$	0.8	1.2	$\cdots$	$\cdots$	5.0
Charmless B	1.25	1.77	0.35	4.53	2.01	0.97	$\cdots$	0.51	1.75
Total	2.99	$+3.33$ -3.56	4.41	$+6.51$ -6.48	$+4.08$ -4.06	2.95	$+3.87$ -3.86	5.03	$+43.09$ -42.87

continuum, we conservatively assign its $\mathcal{A}_{CP}$ value as the systematic uncertainty: this is 0.66×10^{-2} for $B^+ \to \pi^+\pi^0$ and 0.63×10^{-2} for $B^+ \to K^0\pi^+$. With regard to the detector bias for h^0K^+ modes, a sizable number of protons are included due to p-K misidentification in continuum events. Therefore, the possible bias is more reliably estimated using $D_s^+ \to \phi(K^+K^-)\pi^+$ and $D^0 \to K^-\pi^+$ samples [29] and is found to be $(+0.33 \pm 0.19) \times 10^{-2}$; we correct the $\mathcal{A}_{CP}$ values for the bias and assign 0.19×10^{-2} as the systematic uncertainty on $\mathcal{A}_{CP}$. For the bias of the charged kaon and pion identification in the $K^+\pi^-$ mode, we shift the $\mathcal{A}_{CP}$ value by -0.33×10^{-2} and quote 0.67×10^{-2} as the systematic uncertainty for the residual bias. For $\bar{K}^0K^+$ and $K^0\pi^+$ modes, we shift $\mathcal{A}_{CP}$ further for the measured CP asymmetry induced by the SM $K^0 - \bar{K}^0$ mixing: $\mathcal{A}_{CP}(K^0) = (+0.332 \pm 0.006)\%$ [19]. The quadratic sum of the fitting and bias uncertainties gives the total $\mathcal{A}_{CP}$ systematic error, which ranges from 0.002 to 0.007. Compared to our previous measurement of $\mathcal{A}_{CP}(K^+\pi^-)$ [1], the current result, $\mathcal{A}_{CP}(K^+\pi^-) = -0.069 \pm 0.014 \pm 0.007$, differs by 0.025 due to a smaller measured central value in the newest data set of $237 \times 10^6 B\bar{B}$ pairs. Aside from this difference, the measurement is consistent with our previous publication and other experimental results [2,30,31]. Furthermore, the updated difference of CP asymmetries $\Delta\mathcal{A}_{K\pi} = \mathcal{A}_{CP}(K^+\pi^0) - \mathcal{A}_{CP}(K^+\pi^-)$ is given by $+0.112 \pm 0.027 \pm 0.007$ with significance of 4.0σ; this confirms our earlier result, as evident in Fig. 3.

The ratios of partial widths for $B \to K\pi$ and $B \to \pi\pi$ can be used to search for NP [10–12]. These ratios are obtained from the measurements listed in Table I. The ratio of charged to neutral B meson lifetime, $\tau_{B^+}/\tau_{B^0} = 1.079 \pm 0.007$ [19], is used to convert branching fraction ratios into partial width ratios (see Table III). The total uncertainties are reduced because of the cancellation of common systematic uncertainties. These ratios are compatible with SM expectations [9–12] and supersede our

previous results [6]. The partial widths and CP asymmetries are used to test the violation of a sum rule [32] given by $\mathcal{A}_{CP}(K^+\pi^-) + \mathcal{A}_{CP}(K^0\pi^+)\frac{\Gamma(K^0\pi^+)}{\Gamma(K^+\pi^-)} - \mathcal{A}_{CP}(K^+\pi^0) \times \frac{2\Gamma(K^+\pi^0)}{\Gamma(K^+\pi^-)} - \mathcal{A}_{CP}(K^0\pi^0)\frac{2\Gamma(K^0\pi^0)}{\Gamma(K^+\pi^-)} = 0$; the sum is found to be $-0.270 \pm 0.132 \pm 0.060$ (1.9σ significance), using the results in Tables I and III and $\mathcal{A}_{CP}(K^0\pi^0) = +0.14 \pm 0.13 \pm 0.06$ [16]; this is still compatible with the SM prediction. All of these results provide useful constraints to NP models and our uncertainties are now comparable with those of the corresponding theoretical calculations.

In conclusion, we have measured the branching fractions and direct CP asymmetries for $B \to K\pi$, $\pi\pi$ and KK decays using $772 \times 10^6 B\bar{B}$ pairs, which is the final data set at Belle. We confirm a large $\Delta\mathcal{A}_{K\pi}$ value with the world's smallest uncertainty. Including this result, the
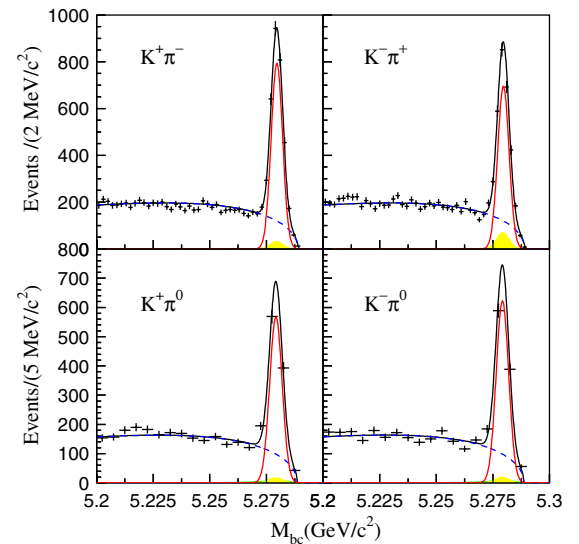

FIG. 3 (color online).   The M_{bc} distributions for $B^0/\bar{B}^0 \to K^\pm\pi^\mp$ (top) and $B^\pm \to K^\pm\pi^0$ (bottom). The selections for fit projections and PDF component descriptions are identical to those described in Fig. 1.

TABLE III. Partial width ratios of $B \to K\pi$ and $\pi\pi$ decays. The errors are quoted in the same manner as in Table I.

Modes	Ratio
$2\Gamma(K^+\pi^0)/\Gamma(K^0\pi^+)$	$1.053 \pm 0.034 \pm 0.052$
$\Gamma(K^+\pi^-)/2\Gamma(K^0\pi^0)$	$1.033 \pm 0.052 \pm 0.057$
$2\Gamma(K^+\pi^0)/\Gamma(K^+\pi^-)$	$1.171 \pm 0.036 \pm 0.055$
$\Gamma(K^+\pi^-)/\Gamma(K^0\pi^+)$	$0.899 \pm 0.026 \pm 0.030$
$\Gamma(\pi^+\pi^-)/\Gamma(K^+\pi^-)$	$0.252 \pm 0.011 \pm 0.009$
$\Gamma(\pi^+\pi^-)/2\Gamma(\pi^+\pi^0)$	$0.464 \pm 0.028 \pm 0.032$
$\Gamma(\pi^+\pi^0)/\Gamma(K^0\pi^0)$	$0.562 \pm 0.037 \pm 0.032$
$2\Gamma(\pi^+\pi^0)/\Gamma(K^0\pi^+)$	$0.490 \pm 0.024 \pm 0.033$

current world average is $+0.124 \pm 0.022$ (5.6σ significance) [33]. We find no significant deviation from SM expectations on the partial width ratios and the $\mathcal{A}_{CP}(K\pi)$ sum rule, and these measurements continue to constrain the parameter space for NP. We report a new upper limit for $B^0 \to K^+K^-$ that is improved by a factor of two over the current most restrictive limit [6] and is consistent with the latest LHCb result [31]. Compared to previous studies, all systematic uncertainties are decreased, including tracking, kaon/pion identification, K_S^0 reconstruction efficiencies, and the likelihood ratio requirement. The inclusion of the three-dimensional fit and improvements in systematic studies have substantially reduced the uncertainties for all channels and have increased the effective size of the data set. The uncertainties for partial width ratios are all improved, especially for R_c (by a factor of 1.6) and R_n (by a factor of 1.4).

[1] S. W. Lin *et al.* (Belle Collaboration), Nature (London) **452**, 332 (2008).

[2] J. P. Lees *et al.* (*BaBar* Collaboration), arXiv:1206.3525.

[3] B. Aubert *et al.* (*BaBar* Collaboration), Phys. Rev. D **76**, 091102 (2007).

[4] C.-W. Chiang, M. Gronau, J. L. Rosner, and D. A. Suprun, Phys. Rev. D **70**, 034020 (2004); Y.-Y. Charng and H.-n. Li, Phys. Rev. D **71**, 014036 (2005).

[5] A. J. Buras, R. Fleischer, S. Recksiegel, and F. Schwab, Nucl. Phys. **B697**, 133 (2004); S. Baek and D. London, Phys. Lett. B **653**, 249 (2007); W.-S. Hou, H.-n. Li, S. Mishima, and M. Nagashima, Phys. Rev. Lett. **98**, 131801 (2007); M. Imbeault, S. Baek, and D. London, Phys. Lett. B **663**, 410 (2008); S. Khalil, A. Masiero, and H. Murayama, Phys. Lett. B **682**, 74 (2009).

[6] S.-W. Lin *et al.* (Belle Collaboration), Phys. Rev. Lett. **99**, 121601 (2007); **98**, 181804 (2007).

[7] B. Aubert *et al.* (*BaBar* Collaboration), Phys. Rev. Lett. **97**, 171805 (2006); Phys. Rev. D **75**, 012008 (2007).

[8] A. Bornheim *et al.* (CLEO Collaboration), Phys. Rev. D **68**, 052002 (2003).

[9] H.-n. Li, S. Mishima, and A. I. Sanda, Phys. Rev. D **72**, 114005 (2005).

[10] A. J. Buras, R. Fleischer, S. Recksiegel, and F. Schwab, Eur. Phys. J. C **45**, 701 (2006).

[11] T. Yoshikawa, Phys. Rev. D **68**, 054023 (2003); S. Mishima and T. Yoshikawa, Phys. Rev. D **70**, 094024 (2004).

[12] M. Gronau and J. L. Rosner, Phys. Lett. B **572**, 43 (2003).

[13] The inclusion of the charge-conjugate decay is implied, unless explicitly stated otherwise.

[14] A. Abashian *et al.* (Belle Collaboration), Nucl. Instrum. Methods Phys. Res., Sect. A **479**, 117 (2002).

[15] S. Kurokawa and E. Kikutani, Nucl. Instrum. Methods Phys. Res., Sect. A **499**, 1 (2003), and other papers included in this volume.

[16] M. Fujikawa *et al.* (Belle Collaboration), Phys. Rev. D **81**, 011101 (2010).

[17] K.-F. Chen *et al.* (Belle Collaboration), Phys. Rev. D **72**, 012004 (2005).

[18] G. C. Fox and S. Wolfram, Phys. Rev. Lett. **41**, 1581 (1978); The modified moments used in this paper are described in S. H. Lee *et al.* (Belle Collaboration), Phys. Rev. Lett. **91**, 261801 (2003).

[19] J. Beringer *et al.* (Particle Data Group), Phys. Rev. D **86**, 010001 (2012).

[20] In the previous publications, a tighter cut is used for the low statistics channel to suppress the high background-level. Therefore, the luminosity gain for K^+K^-, which comes from the three-dimensional fit, is substantially larger than $K^+\pi^-$ and $K^+\pi^0$ for the same $\mathcal{R}$ cut.

[21] T. Skwarnicki, DESY Report No. F31-86-02, 1986 (unpublished).

[22] The sample for ΔE width calibration in $h\pi^0$ is D^0 decays to $K^-\pi^+\pi^0$ with a $p_{\pi^0} > 1.5$ GeV/c requirement; the sample for $K^0\bar{K}^0$ calibration is D^0 decays to $\pi^+\pi^-K^0$ with a requirement on $p_{K^0} > 1.0$ GeV/c.

[23] The control samples used for calibrating the means as well as widths for M_{bc} or $\mathcal{R}'$, the means for ΔE, and for estimating systematic uncertainties due to the likelihood ratio requirement are: (a) $B^+ \to \bar{D}^0(K^+\pi^-)\pi^+$ for the h^+h^-, $K^0\pi^+$, and $\bar{K}^0K^+$ channels,

(b) $B^+ \to \bar{D}^0(K^+\pi^-\pi^0)\pi^+$ for the $h\pi^0$ channels, and (c) $B^+ \to \bar{D}^0(K^+\pi^-K^0)\pi^+$ for $K^0\bar{K}^0$.

[24] H. Albrecht *et al.* (ARGUS Collaboration), Phys. Lett. B **241**, 278 (1990).

[25] See Supplemental Material at http://link.aps.org/supplemental/10.1103/PhysRevD.87.031103 for fit projections in $\mathcal{R}'$.

[26] The reconstruction efficiency of $B^0 \to K^0\bar{K}^0$ channel accounts for the $K_S^0 K_S^0$ decay, which corresponds to half of the $B^0 \to K^0\bar{K}^0$ contribution. The $\varepsilon \times \mathcal{B}_s$ term has already considered this.

[27] E. Barberio and Z. Was, Comput. Phys. Commun. **79**, 291 (1994); P. Golonka and Z. Was, Eur. Phys. J. C **45**, 97 (2006). We use PHOTOS version 2.13 allowing the emission of up to two photons, with an energy cut-off at 1% of the total energy available for photon emission (i.e., approximately 26 MeV for the first emitted photon). PHOTOS also takes into account interference between radiation from charged final-state particles.

[28] The number of $B\bar{B}$ pairs is estimated based on the number of hadronic events measured in on-resonance data, subtracting the number of hadronic events in off-resonance data. The off-resonance values are corrected for efficiency differences between on- and off-resonance configurations, as well as luminosity scaling. After the subtraction, systematic uncertainty arises from the luminosity scaling, which is estimated using the $e^+e^- \to \mu^+\mu^-$ events.

[29] B. R. Ko *et al.* (Belle Collaboration), Phys. Rev. Lett. **104**, 181602 (2010); K. Sakai *et al.* (Belle Collaboration), Phys. Rev. D **82**, 091104 (2010).

[30] T. Aaltonen *et al.* (CDF collaboration), Phys. Rev. Lett. **106**, 181802 (2011).

[31] S. Perazzini *et al.* (LHCb collaboration), Nuovo Cimento Soc. Ital. Fis. C **034N06**, 292 (2011); R. Aaij *et al.* (LHCb collaboration), Phys. Rev. Lett. **108**, 201601 (2012); R. Aaij *et al.* (LHCb collaboration), J. High Energy Phys. 10 (2012) 037.

[32] M. Gronau, Phys. Lett. B **627**, 82 (2005).

[33] Y. Amhis *et al.* (Heavy Flavor Averaging Group), arXiv:1207.1158 and online update at http://www.slac.stanford.edu/xorg/hfag.